ACS chemical biology

ARTICLE

Discovery of Specific Flavodoxin Inhibitors as Potential Therapeutic Agents against *Helicobacter pylori* Infection

Nunilo Cremades[†,‡], Adrián Velázquez-Campoy[‡,§], Marta Martínez-Júlvez[†,‡], José L. Neira[‡,¶], Inmaculada Pérez-Dorado[∥], Juan Hermoso[∥], Pilar Jiménez[⊥], Angel Lanas[⊥], Paul S. Hoffman[○], and Javier Sancho[†,‡,*]

[†]Departamento de Bioquímica y Biología Molecular y Celular, Facultad de Ciencias, Universidad de Zaragoza, Spain, [‡]Biocomputation and Complex Systems Physics Institute (BIFI)-Unidad Asociada al IQFR-CSIC, 50009 Zaragoza, Spain, [§]Fundación Aragón I+D (ARAID-BIFI), Diputación General de Aragón, Spain, [¶]Instituto de Biología Molecular y Celular, Universidad Miguel Hernández, 03202 Elche, Spain, [∥]Grupo de Crystalografía Macromolecular y Biología Estructural, Instituto de Química-Física Rocasolano, CSIC, Serrano 119, 28006 Madrid, Spain, [⊥]IACS, CIBERehd, University of Zaragoza, Spain, and [○]Department of Medicine, Division of Infectious Diseases and International Health, University of Virginia, Charlottesville, Virginia 22908

ABSTRACT *Helicobacter pylori* establishes life-long infections in the gastric mucosa of over 1 billion people worldwide. In many cases, without specific antimicrobial intervention, *H. pylori* infected individuals will develop type B gastritis, chronic peptic ulcers and, more rarely, gastric neoplasias. Conventional antimicrobial therapy has been complicated by dramatic increases in resistance to macrolides, metronidazole and fluoroquinolones. Here, we report the development of novel therapeutics that specifically target the unique flavodoxin component of an essential metabolic pathway of *H. pylori*. With the use of high-throughput screening methodology, we have tested 10,000 chemicals and have identified 29 compounds that bind flavodoxin, four of which interrupted *in vitro* electron transfer to flavodoxin physiological partners. Three of these compounds are bactericidal and promisingly selective for *H. pylori*. The minimal inhibitory concentrations of two of them are 10 times lower than their minimal cytotoxic concentrations for HeLa cells. Importantly, neither of the four inhibitors is toxic for mice after administration of 1–10 mg kg^{-1} doses twice a day for 5 days. Enzymatic, thermodynamic and structural characterization of the inhibitor–flavodoxin complexes suggests these compounds could act by modifying the redox potentials of flavodoxin. These newly discovered inhibitors represent promising selective leads against the different diseases associated to *H. pylori* infection.

*Corresponding author, jsancho@unizar.es.

Received for review July 14, 2009 and accepted September 2, 2009.

Published online September 2, 2009

10.1021/cb900166q CCC: $40.75

Despite 25 years of antimicrobial intervention since *Helicobacter pylori* (Hp) infection was first linked with gastritis and gastroduodenal ulcers (*1*), over a billion people worldwide remain infected. Life-long infection of the gastric mucosa is also associated with increased risk of mucosa-associated lymphoid tissue (MALT) lymphoma (*2, 3*) and gastric adenocarcinoma (*4*). While in developed countries the incidence of Hp infection has diminished to 20–30% of the population, the prevalence of infection in developing countries is high or extremely high (*5*) and there is little hope it will decrease in the short-medium time, since useful vaccines seem far from being available (*6, 7*). Furthermore, in many of these countries, eradication therapies face the problems of high cost, high frequency of strains resistant to available antibiotics, and/or high reinfection rates due to poor socioeconomical and sanitation development. Aside from improving sanitation, there is an urgent need for inexpensive medications that can be routinely used to treat this infection and reduce the impact of the disease worldwide.

The current conventional treatment for patients with Hp infection consists of two front line broad spectrum antibiotics, such as amoxicillin and clarithromycin, together with a proton pump inhibitor (*8*). While these combinations, as well as others containing metronidazole and tetracycline, have achieved eradication rates as high as 95%, the success rates have fallen dramatically as a result of increasing drug resistance (*9–12*) (*13*), and much effort is currently spent on developing

salvage eradication therapies to treat infections caused by multiply resistant strains (*14, 15*).

Several groups have tried to develop narrow spectrum antimicrobials against Hp and have indeed identified many selective targets in this organism (*16*). One of them is flavodoxin, whose function is essential for Hp viability (*17, 18*). Flavodoxins (*19*) are microbial electron carriers, involved in a variety of reactions, that bear one molecule of flavin mononucleotide (FMN) as a noncovalently bound redox cofactor. The flavodoxin from Hp (Hp-Fld) couples the oxidative decarboxylation of pyruvate to the production of reduced nicotinamide adenine dinucleotide phosphate (NADPH) by shuttling electrons from the pyruvate:ferredoxin oxidoreductase complex (PFOR) (*17, 20*) to flavodoxin:quinone reductase (FqrB) (*16, 21*). Each of these three proteins is essential for Hp survival (*16, 17, 20, 22*). From a structural point of view, Hp-Fld is peculiar in that a tryptophan residue typically involved in cofactor binding in many flavodoxins is replaced by an alanine (*17*), which creates a distinct pocket near the cofactor (Figure 1, panels a and b). Our preliminary analysis of more than 200 flavodoxin sequences available in UniProtKB (not shown) indicates that such replacement only takes place in *H. pylori*, *Helicobacter acinonychis* (both able to infect the stomach) and *Treponema pallidum*. In contrast, *Helicobacter hepaticus*, a nongastric species, displays a tyrosine residue. It is possible that the replacement observed in Hp be a functional requirement for *Helicobacter* species able to infect the stomach. Flavodoxin is not present in humans, but it is homologous to one domain of human P450 cytochrome reductase. This domain bears a bulky tyrosine residue at the critical position, and as it happens in the vast majority of flavodoxins, there is no pocket near the cofactor (Figure 1, panel d). The Hp-Fld pocket is thus an inviting feature for developing selective inhibitors that could interfere with electron transfer by either modifying the redox potentials, or impairing the interaction with partner proteins.

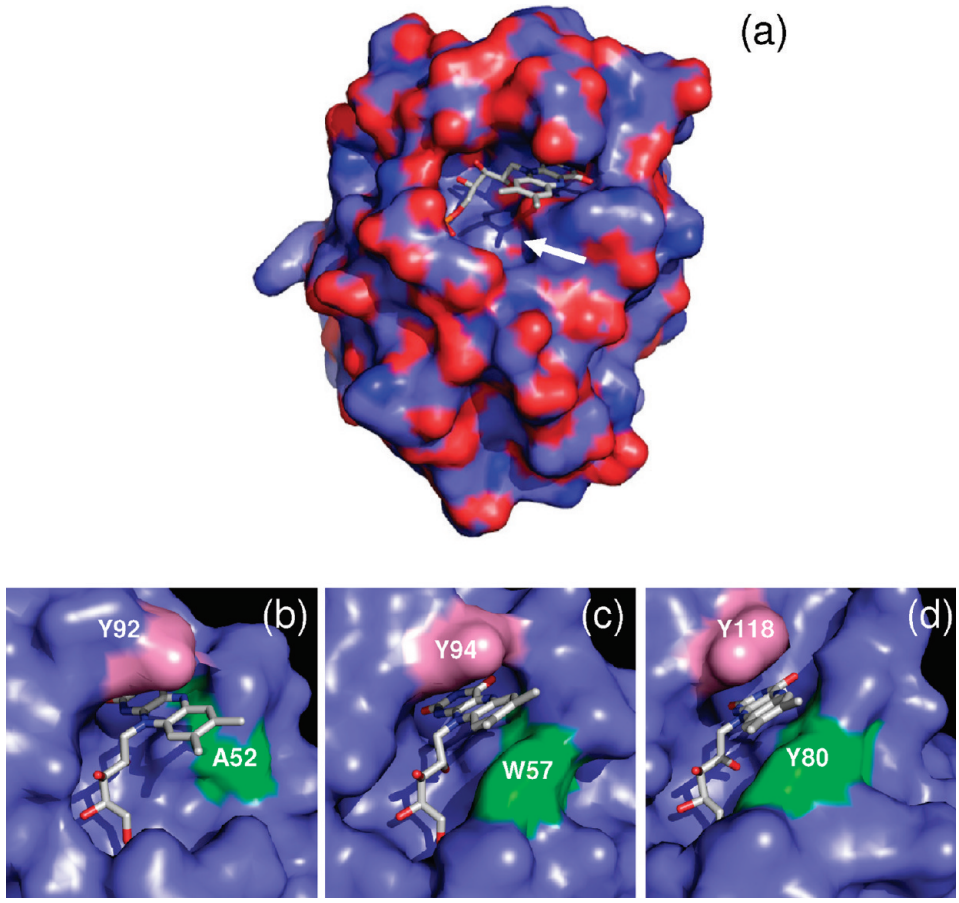

Figure 1. Molecular surface of Hp-Fld and of homologous proteins. a) Molecular surface of Hp-Fld colored according to atom type and showing the FMN cofactor (sticks). The cavity close to the cofactor that appears suitable for therapeutical intervention is highlighted with a white arrow. b) Close view of the active site. The presence in Hp-Fld of an alanine residue where most flavodoxins carry a bulky one creates a pocket close to the redox cofactor that can be filled by small organic molecules in order to block flavodoxin function. c) The active site of *Anabaena* PCC7119 flavodoxin is shown here to highlight the presence of a conserved tryptophan residue instead of an alanine. d). Human P450 citochrome reductase contains a domain homologous to bacterial flavodoxin, but no pocket appears near the FMN cofactor due to the presence of a tyrosine residue.

In a recent study (*18*), we identified, from simple reasoning, small molecules that are able to bind to the Hp-Fld pocket. However, they all displayed low affinities, with dissociation constants in the millimolar range.

This prompted us to look for more efficient high-throughput screening (HTS) strategies to identify stronger binders that could exert inhibitory effects. To that end, we have implemented a HTS method that detects binders from the stabilizing effect they exert on the target protein (*23–30*), a procedure that has been successfully used recently to identify pharmacological chaperones of a defective human enzyme (*31*). Accordingly, Hp-Fld has been screened against a chemical library of 10,000 compounds of high chemical diversity and good pharmacokinetic properties. Twenty-nine binders with affinities in the micromolar range have been identified, four of which inhibit flavodoxin function *in vitro*. Three of these flavodoxin inhibitors are bactericidal agents specific for Hp. The toxicity of two of them in HeLa cells is mild (with minimal cytotoxic concentrations (MCC) 10 times higher than the corresponding minimal inhibitory concentrations (MIC)) and their oral administration to mice does not seem to induce renal or hepatic toxicity. These new inhibitors constitute promising candidates to develop new specific antibiotics against *H. pylori*.

RESULTS AND DISCUSSION

A General, Simple HTS Method To Identify Binders of Target Proteins: Identification of Binders to *H. pylori* Flavodoxin. Drug discovery using cell-based assays (*32*) is advantageous in that the compounds identified are already effective on a specific cell-line, but it offers little insight into mechanisms of action at a molecular level, which may slow down subsequent hit-to-lead optimization steps. We have implemented a target-based and affinity-based screening method that can in principle identify compounds that bind to any purified protein target. Because preferential binding of any compound to the native state of any protein increases protein stability, simple measurements of melting temperatures (T_m) in protein unfolding curves recorded in the presence of ligands constitute an easy way to detect binders (*31*).

Hp-Fld presents a complex four-state thermal unfolding equilibrium, with two partially unfolded intermediate states (*33*). However, following the unfolding by the increase in fluorescence associated to cofactor release gives rise to curves that resemble those of simple two-state equilibria (*33*). The inflection point of these curves is the melting temperature (T_m) and roughly corresponds to the temperature at which half of the Hp-Fld molecules are in the native state and the other half are non-functional folding intermediates deprived of cofactor. Binding of ligands to native flavodoxin increases its stability relative to that of the intermediates, which causes an increase in T_m. In standard thermal unfolding analysis (non-HTS), T_m values are determined by fitting single curves to the theoretical equations corresponding to the specific unfolding mechanism previously determined for a given protein. However, fitting hundreds of curves in this way is not very effective due to the need to anticipate reasonable initial estimates (both thermodynamic and spectroscopic ones). Therefore, we have developed homemade software that allows a quick and fairly accurate estimation of the melting temperature of the several hundred curves recorded in each unfolding experiment (see Methods). With this method, 10,000 chemically diverse compounds were screened, 29 of which gave rise to $\Delta T_m \geq 3$ °C and were selected for inhibitory assays. A representative example of thermal screening results corresponding to a deconvolutionary experiment where compounds present in some of the positive wells were tested individually (see Methods) is shown (Figure 2, panel a). In the figure, one of the 29 compounds that was finally identified as a Hp-Fld inhibitor, inhibitor III, is marked with an asterisk. In general, the thermal unfolding curves obtained in the HTS fluorimeter agree well with those recorded in a conventional one, as indicated by the superimposition of equivalent curves (Figure 2, panel b). This figure shows that, in the presence of 100 μM inhibitor III, the HTS flavodoxin unfolding curve is clearly shifted to higher temperatures, indicating that a strong complex is formed between the protein and inhibitor III. On the other hand, the fact that inhibitor III lowers the fluorescence of native flavodoxin (see data at low temperatures) suggests that the inhibitor binds close to the fluorescent FMN cofactor, thus quenching it.

***In Vitro* Testing of Flavodoxin Binders for Inhibition of an Essential Electron Transfer Pathway.** In a recent study (*21*), it was shown that one physiological function of Hp-Fld is the transfer of electrons arising from the PFOR-mediated oxidative decarboxylation of pyruvate to FqrB, an oxidoreductase which reduces nicotinamide adenine dinucleotide phosphate ($NADP^+$) (Figure 3, panel a). To identify Hp-Fld inhibitors, the 29 binders found in the HTS were tested *in vitro* in a coupled enzymatic assay in the presence of Hp-Fld and its redox partners PFOR and FqrB. Functional Hp-Fld is revealed in this assay by an increase in absorbance at 340 nm due

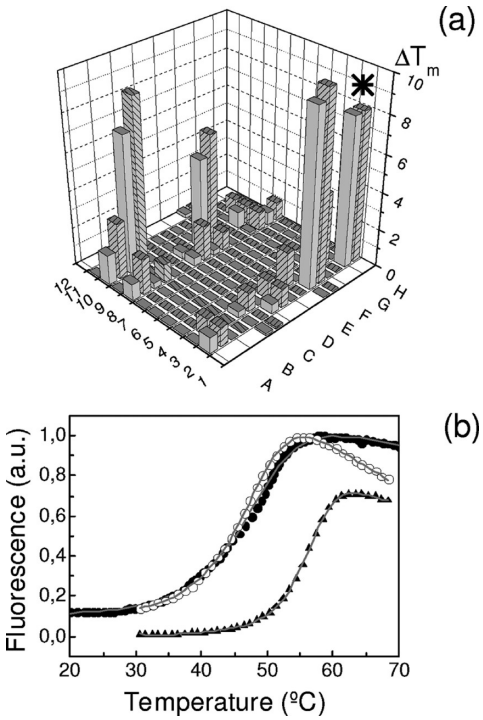

Figure 2. High-throughput screening for Hp-Fld inhibitors by thermal upshift assays. a) Compound-induced increases in T_m for Hp-Fld unfolding detected in a typical assay performed in a 96-well plate (columns labeled in numbers 1–12 and rows in letters A–H). Columns 1 and 12 of the plate were only used for control experiments with protein in absence of compound. Gray bars represent ΔT_m values calculated using a mid point analysis, while striped gray bars are ΔT_m calculated using an inflection point method (see Methods). One of the active compounds identified (inhibitor III) is labeled with an asterisk. b) Raw Hp-Fld thermal unfolding curves in absence (filled circles) and presence of 100 μM of inhibitor III (filled triangles) compared with an unfolding curve obtained in absence of inhibitor in a common spectrofluorimeter (empty circles). Continuous lines are fits to a two-state unfolding model. The observed quenching of FMN fluorescence at low temperatures exerted by inhibitor III suggests that it binds close to the FMN cofactor.

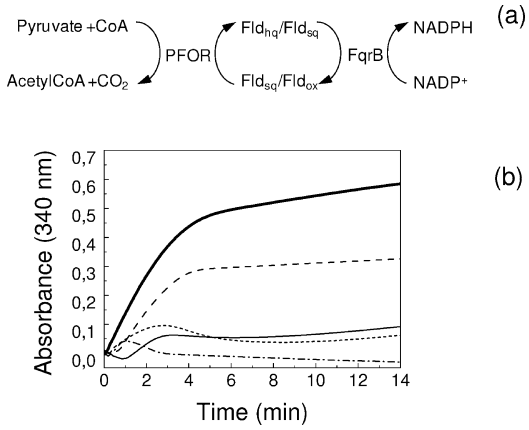

Figure 3. Electron transfer inhibition assay. a) Scheme of the coupled reaction used to determine flavodoxin functionality. This reaction reconstitutes the physiological pathway by which *H. pylori* derives electrons generated in the oxidative decarboxylation of pyruvate toward the synthesis of NADPH. Flavodoxin can exist in three redox forms: oxidized, Fldox; semiquinone (one electron-reduced), Fldsq; and hydroquinone (two electron-reduced), Fldhq. The three redox forms are active in the coupled reaction. b) Kinetics of NADPH formation followed by absorbance at 340 nm in absence of inhibitors (thick line) and in presence of 70 μM inhibitor I (thin line), 81 μM inhibitor II (dashed line), 78 μM inhibitor III (dotted line) and 73 μM inhibitor IV (dot-dashed line). The concentrations of the compounds were chosen so that the DMSO concentration was identical in all the experiments. The same DMSO concentration was used in absence of compounds as control. PFOR and FqrB concentrations were approximately 0.4 and 0.2-μM, respectively; while that of Hp-Fld was 3–5 μM.

to NADPH production. Inhibitory assays were performed with 60–80 μM compound and 3–5 μM Hp-Fld. The coupled reaction is almost insensitive to the dimethyl sulphoxide (DMSO) concentration present in the assay (5%). Four out of the 29 apparently binding compounds tested decreased markedly the rate of NADPH formation in pseudoanaerobic conditions (not shown), and they were subsequently reassayed in strict anaerobiosis. The kinetic curves obtained in anaerobiosis (Figure 3, panel b) confirm that the four compounds inhibit the reduction of $NADP^+$, albeit one of them (inhibitor II) only produces a partial inhibition in this assay. The chemical structures of the four inhibitors are shown (Figure 4). All of them are fairly simple nitroaromatic compounds.

Affinity of Flavodoxin/Inhibitor Complexes. The binding of the four inhibitors to Hp-Fld was inferred from their up-shifting effect on the melting temperature of the protein in the HTS assays. From the changes in T_m values, the affinity of the complexes can be estimated to be in the micromolar range of dissociation constants (Table 1). To obtain more accurate values of the affinities, the binding of the inhibitors to Hp-Fld was directly monitored by ITC. In all cases, complexes of a 1:1 stoi-

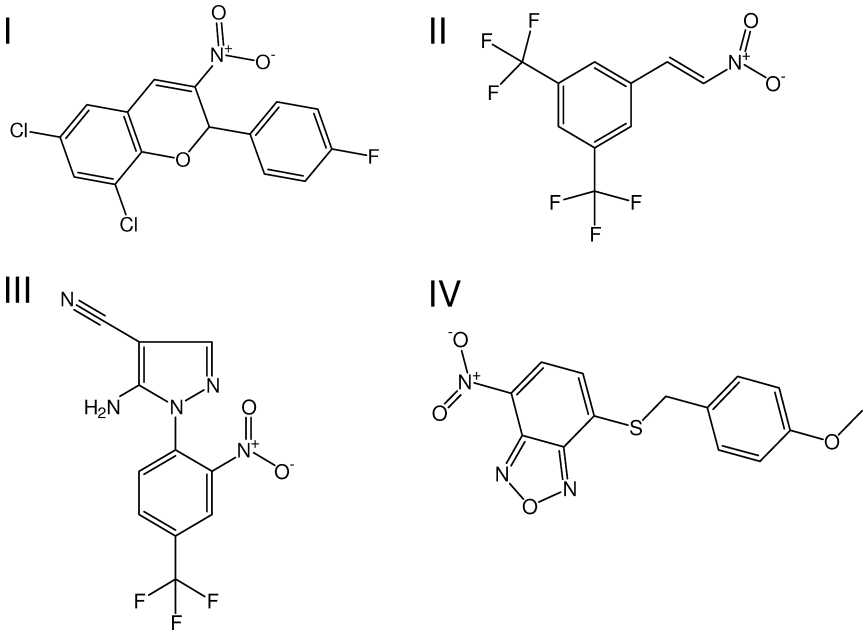

Figure 4. Chemical structure of the four inhibitors identified. I, 6,8-Dichloro-2-(4-fluorophenyl)-3-nitro-2*H*-chromene; II, 1-(2-nitrovinyl)-3,5-di(trifluoromethyl)benzene; III, 5-amino-1-[2-nitro-4-(trifluoromethyl)phenyl]-1*H*-pyrazole-4-carbonitrile; IV, 4-[(4-methoxybenzyl)thio]-7-nitro-2,1,3-benzoxadiazole.

chiometry were observed, the dissociation constants of which ranked from 0.6 to 8 μM (Table 1). The two-step HTS strategy based in first screening for binders and then testing for inhibitory properties produced four Hp-Fld inhibitors with an affinity for the target protein sufficiently high so as to consider them further as potential hits for drug development against Hp.

TABLE 1. Affinities of flavodoxin/inhibitor complexes

	Thermal upshift assay			ITC	
Inhibitor	ΔT_m[a]	K_D[b] μM	ΔG_b kcal mol^{-1}	K_D[c] μM	ΔG_b kcal mol^{-1}
I	7	12.2	−6.7	1.6 ± 0.3	−7.9 ± 0.1
II	3	65.2	−5.7	8 ± 2	−6.9 ± 0.2
III	8	8.1	−7.0	0.6 ± 1	−8.5 ± 0.7
IV	11	3.5	−7.4	3 ± 1	−7.5 ± 0.1

[a] T_m values calculated as described in the high-throughput screening section of the Methods. [b] K_D values extrapolated at 25.0 °C. [c] K_D values determined at 25.0 °C

Inhibition of *H. pylori* Culture Growth: Bactericidal Effect of Three of the Four Inhibitors. To determine whether the inhibitors were biologically active against the target bacteria, microdilution MIC testing was performed. As seen in Table 2, inhibitor III was bacteriostatic against *H. pylori* and *Campylobacter jejuni*. The most potent activity was noted with inhibitor I followed by inhibitor II. With the exception of inhibitor III, all of the compounds were more active that nitazoxanide, the noncompetitive inhibitor of PFOR (*34*), and less active than ampicillin.

To determine whether the inhibitors were bactericidal, kill curves were performed at 2× the MICs listed in Table 2. As seen in Figure 5, inhibitor III was only bacteriostatic against both strains of Hp tested. While not depicted, similar results were obtained for this compound with *C. jejuni*. The other three inhibitors were bactericidal, with inhibitors II and I being the most toxic and inhibitor IV the least for Hp. The bactericidal effect of these compounds is well within a therapeutic range for treatment of infections caused by *H. pylori* (*35*). Further testing will be required to demonstrate selectivity, but the prospects of a narrow spectrum are good. Our preliminary data (Table 2) indicate that the inhibitors do not impair the growth of distant bacteria, except inhibitor I which shows some effect against *Staphylococcus*.

Toxicity of the Four Inhibitors in Human Cell Lines and in Mice. The toxicity of the inhibitors for HeLa cells was determined by visual quantitation of cell damage after 24 h and, additionally, by an LDH liberation assay (see Supplemental Methods). Since it is known that the sensitivity of different methods in current use to detect cell damage is not the same (*36, 37*), it seems appropriate to report as minimal cytotoxic concentrations (MCC) the lowest ones provided for a given compound by the different methods used. In this way, underestimation of cytotoxicity is more effectively avoided. As seen in Supplementary Table S1, inhibitor concentrations producing 50% cell lysis tend to be lower when determined from visual inspection than when calculated from LDH leakage. Thus, we have chosen to report here as MCC those results derived from the visual inspection method.

TABLE 2. Minimal Inhibitory Concentrations[a]

		Species											
		H. pylori 1061		*H. pylori 26695*		*C. jejuni*		*Escherichia coli* DH5α		*Staphylococcus epidermidis*		*Staphylococcus aureus (ATCC1228)*	
Inhibitor	MW	μg mL^{-1}	μM	μg mL^{-1}	μM	μg mL^{-1}	μM	μg mL^{-1}	μM	μg mL^{-1}	μM	μg mL^{-1}	μM
I	338	0.25	0.7	0.125	0.4	2	6	>32	>95	4	12	2	6
II	285	0.5	1.8	0.25	0.9	2	7	>32	>112	>32	>112	>32	>112
III	297	8	27	16	54	8	27	>32	>108	>32	>108	>32	>108
IV	317	2	6	1	3	1	3	>32	>101	>32	>101	>32	>101
NTZ[b]	307	4	13	1	3	8	26						
Amp.[b]	349	<0.025	<0.07	<0.025	<0.07	0.092	0.3						
DMSO		-		-		-							

[a]Minimal inhibitory concentration represents the drug concentration which inhibits growth of the bacteria. [b]NTZ, nitazoxanide; Amp., ampicillin.

The MCC range from 32 μg mL^{-1}, for the less toxic inhibitor III, to 0.5 μg mL^{-1} for the more toxic inhibitor IV. Of the three bactericidal inhibitors, the least cytotoxic one is inhibitor II, with MCC of 4 μg mL^{-1}, well above its MIC of 0.5–0.25 μg mL^{-1} for Hp. Bactericidal inhibitor I, with MCC of 1 μg mL^{-1} and MIC of 0.25–0.125 μg mL^{-1} seems also promising.

In vivo toxicity of the 4 inhibitors was also tested in mice. After 1 week of treatment with two different doses of each compound tested (mice groups of 4 per dose and compound), no differences were found in a wide range of biochemical parameters including urea, creatinine, liver transaminases, Na^+, Cl^-, K^+, P, Ca^{2+}, bilirubin, amylase, LDH, alkaline phosphatase, albumin, globulin, and total protein amount, when compared to controls (data not shown). Mice were sacrificed at the end of the treatment period and both macroscopic and microscopic examination of different organs including, liver, kidney, lung, heart, stomach and spleen showed no pathological changes.

Structural Analysis of the Flavodoxin:Inhibitor Complexes with Inhibitors III and IV. The promising inhibitory properties of the compounds identified by HTS have prompted us to obtain structural information of their complexes with Hp-Fld. This information may help to understand their mechanisms of action and also to improve their properties by rational redesign. At present, we have solved the crystal structure of the Hp-Fld:inhibitor III complex, and obtained lower resolution information on the same complex and on that with inhibitor IV by NMR (see Supplemental Methods).

The crystal structure of the flavodoxin:inhibitor III complex consists of two flavodoxin monomers (A and B) per asymmetric unit presenting the same overall fold (Figure 6, panel a). Overall, the structure is similar to that of Hp-Fld (rmsd values of 0.451 and 0.407 Å for monomers A and B with respect to uncomplexed flavodoxin, respectively). The prosthetic group in monomer B appears bound in the same configuration than that of uncomplexed Hp-Fld. In contrast, the electron density map for monomer A was broken in the region connecting the isoalloxazine ring with the ribitol-phosphate moiety of the FMN. Besides, the electron density associated

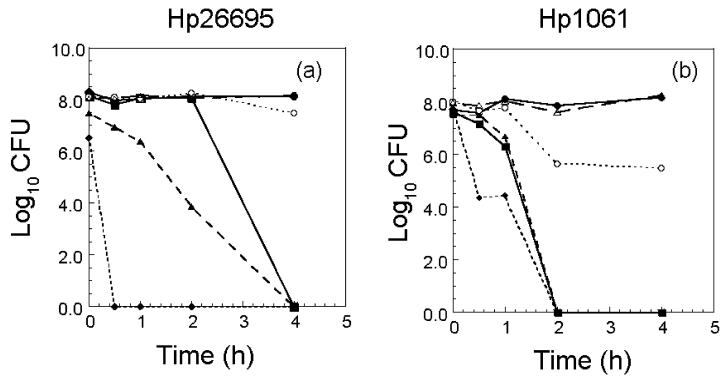

Figure 5. Bactericidal testing of flavodoxin inhibitors against two *H. pylori* strains. a) *H. pylori* strain 26695 and b) *H. pylori* strain 1061. Compounds were tested at MIC or higher as indicated in Table 2. Inhibitor I (▲); II (◆); III (●); IV (■); nitazoxanide (○); and DMSO control (2%) (Δ). CFU = viable count per mL. Inhibitors I, II, and IV are bactericidal against the two *H. pylori* strains, while compound III is only bacteriostatic. Nitazoxanide, a noncompetitive inhibitor of PFOR (21), was also tested for comparison.

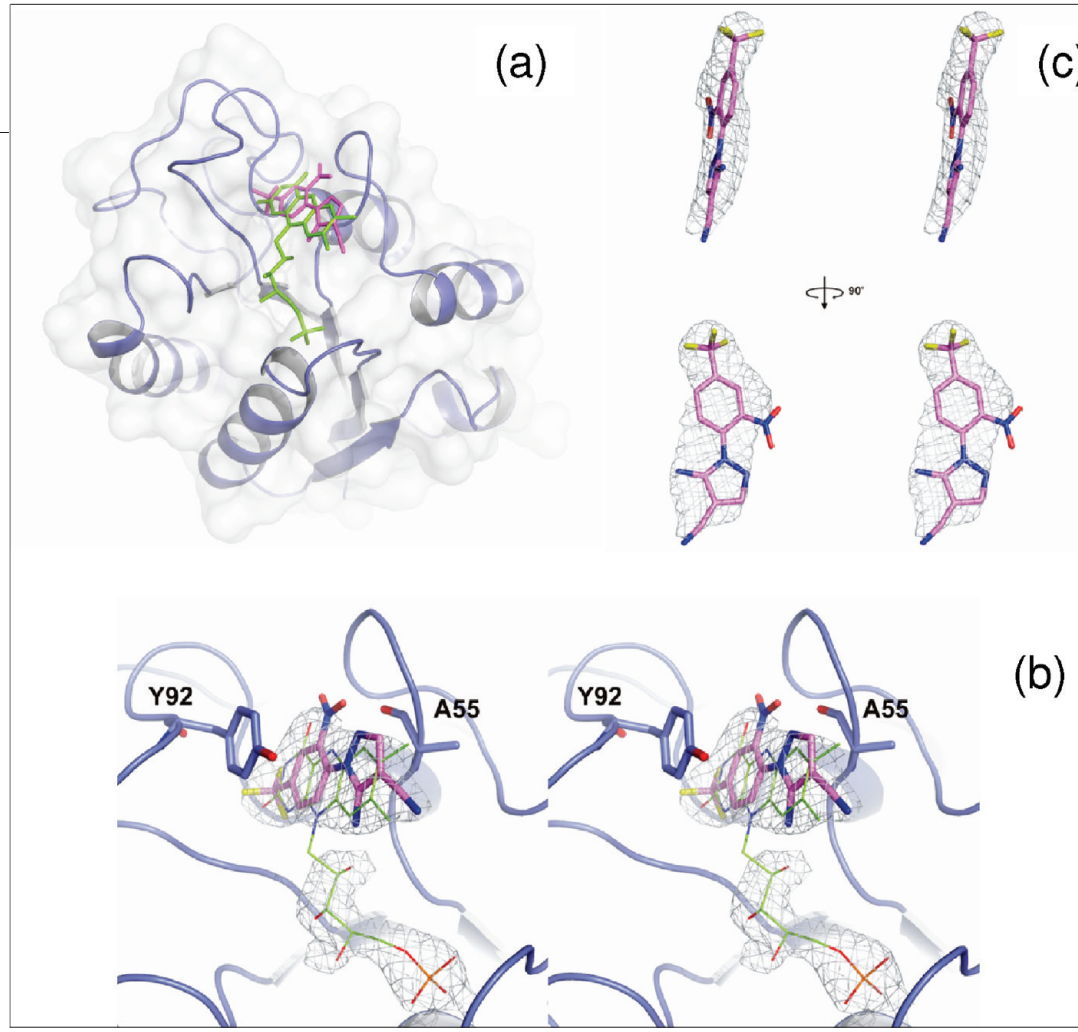

Figure 6. X-ray structure of the *H. pylori* flavodoxin in complex with inhibitor III. a) Structure of the flavodoxin:inhibitor III complex showing the protein secondary structure of the polypeptide chain (blue), and the FMN cofactor (green) and inhibitor III (magenta) in sticks. b) Stereoview of the FMN binding site in monomer A, showing the electron density map (in gray) of FMN (lines) and inhibitor III (sticks). c) Stereoviews of the electron density map observed for the inhibitor, which is represented in sticks.

with the isoalloxazine ring presented strong distortions such as a bulky electron density at one end, which could only be explained by a replacement of the FMN by the inhibitor in some of the flavodoxin molecules in the crystal (Figures 6, panels b and c). The electron density for the putative FMN cofactor was extremely poor and only the phosphate and part of the ribitol were clearly identified. Binding of inhibitor III is accompanied by slight structural rearrangements and it is stabilized by several H-bond interactions formed through its fluorine atoms and its nitro group with Gly58, Asp88, Thr95 and Ala97 and also by hydrophobic interactions between its benzene ring and Thr54, Ala55, Tyr92 and Phe96 (Supplemental Figure S1).

The Hp-Fld:inhibitor III complex has also been investigated in solution by NMR. Inhibitor III did show STD effects with protons of the benzene ring and with one of the NH_2 protons (Supplemental Figure S2), which is consistent with the tight interactions observed in the crystal structure. The Hp-Fld:inhibitor IV complex was similarly probed by NMR using the BIRD sequence (*38*). Our data indicate (not shown) that the aromatic proton of the anixole close to the nitro group showed STD effects, which suggests that the nitro group of inhibitor IV might also be involved in interaction with the protein. These structural results suggest a key role of the nitro group in the binding of these compounds to Hp-Fld.

Possible Mechanisms of Inhibition. Understanding the mechanism of action of the flavodoxin inhibitors may help to improve them. We suggested recently (*39*) that the natural pocket near the redox cofactor of Hp-Fld might be of functional importance either for modulation of the redox potentials of the protein or for allow-

ing its binding to specific redox partners in Hp. Therefore, our working hypothesis was that flavodoxin inhibitors would bind at or close to that pocket. Modification of Hp-Fld redox potentials may be detrimental for function. Epsilon-proteobacteria seem to catalyze reverse electron transport from NADPH to Acetyl-CoA using a novel pathway that utilizes PFOR, Fld and FqrB (*21*), and that could require less negative flavodoxin potentials. Filling the pocket near the flavodoxin FMN cofactor with small molecules could significantly modify Hp-Fld redox potentials so as to disrupt the electron transport route essential for the pathogen. This possibility has not been directly tested due to low solubility and optical interference of the inhibitors. However, the kinetics of flavodoxin reduction by PFOR in the presence of inhibitor III indicate (Supplemental Figure S3, panel b) that the semireduced state of the FMN cofactor is stabilized, suggesting that this inhibitor modifies the redox potentials of Hp-Fld.

An alternative mechanism for flavodoxin inhibition worth considering would be preventing complex formation with its redox partner proteins, PFOR and FqrB. Direct measurement of the affinity of the PFOR:Fld complex is very difficult due to the extreme fragility of the PFOR heterotetramer. However, the electron transfer kinetics of flavodoxin reduction by PFOR recorded in absence and in presence of inhibitors I, II or III, indicate (Supplemental Figure S3, panel a) that oxidized flavodoxin is consumed at very similar rates in all cases, suggesting that the reduction of oxidized flavodoxin by reduced PFOR is not significantly affected by the inhibitors. As for the Fld:FqrB complex, the dissociation constant was determined by ITC (Supplemental Figure S4). The influence of inhibitors I, II and IV on the affinity could not be measured because the DMSO concentration required to keep them in solution affected the stability of FqrB, but the effect of the more soluble inhibitor III could be determined. The affinity of the Hp-Fld with FqrB in the presence of excess inhibitor III (300 μM) was very similar ($K_D = 0.4 \pm 0.3$ μM) to that measured without inhibitor ($K_D = 0.8 \pm 0.1$ μM), indicating inhibitor III does not preclude Fld:FqrB complex formation.

While the available data on the flavodoxin complexes with inhibitors I, II and IV do not allow a proposed inhibition mechanism for these compounds, more data is available for the complex with inhibitor III. It seems that compound III binds initially near the FMN binding site, possibly at the natural pocket nearby (Figure 1, panel a), which is reflected in the quenching of FMN fluorescence and increased protein stability (Figure 2, panel b). In this initial complex, the cofactor is as efficiently reduced to the semiquinone state as in the absence of compound, but the subsequent reduction to the hydroquinone state is slower and takes place to a lower extent (Supplemental Figure S3). This suggests that, although flavodoxin carrying inhibitor III can still bind to FqrB, it might not reduce the enzyme efficiently, which would in turn block NADPH production. In a subsequent step, and according to the X-ray structure available (Figure 6), inhibitor III is able to displace the redox cofactor FMN from its binding site, thus, completely inactivating the redox function of flavodoxin and impairing the essential metabolic pathway connecting pyruvate decarboxylation with NADPH formation in Hp.

In conclusion, micromolar inhibitors of Hp-Fld have been identified in a commercial library of chemically diverse compounds by a simple and general HTS method based on detecting binding to the target protein by monitoring protein stability. The screening method seems quite efficient as judged by its recent success in identifying pharmacological chaperons for a human defective protein (*31*). The four flavodoxin inhibitors identified halt the growth of different Hp strains and three of them are bactericidal at fairly low concentrations. At least two of them show low toxicity toward HeLa cells at doses well above the MICs and do not appear to be toxic for mice at doses recommended for standard antibiotic therapy. The target-oriented approach followed to discover the inhibitors, the structural peculiarities of the targeted protein compared to homologous flavodoxins from other bacteria, and the preliminary activity spectrum of the inhibitors point to these compounds as leads for a new family of specific antibiotics against *H. pylory* infection.

METHODS

Protein Purification and Quantification. Recombinant Hp-Fld was purified as described (*18*) and a mixture of holo and apo forms was obtained. Apo and holoflavodoxin were separated in a MonoQ10 column (FPLC, Amersham) equilibrated in 50 mM Tris-HCl, pH 8, using a 0 to 1 M linear NaCl gradient. Cloning of

the *porGDAB* operon and its expression and purification from *E. coli* have been previously described (*34, 40*).

PFOR was partially purified to around 30%. Further purification was avoided to prevent the disruption of the functional heterotetramer. The protein content of the PFOR samples was determined by the Bradford assay. The recently described FqrB enzyme (*21*) was overexpressed in *E. coli* as a His_6-tag protein and was purified by nickel interaction chromatography (*21, 40*). The purity of the eluted fractions was confirmed by electrophoresis. The extinction coefficient of Hp FqrB in the fully oxidized state was determined as described (*41*) using, for released FAD, an extinction coefficient at 450 nm of 11.3 mM^{-1} cm^{-1}, in 50 mM Tris buffer pH 8. The extinction coefficient of FqrB (at 25 $\pm$ 0.1 °C) at 462 nm is of 10.6 mM^{-1} cm^{-1} in 50 mM Tris buffer pH 8. The same value was obtained in PBS with 10% glycerol, the buffer used to store the protein.

Chemicals. A library of 10,000 small molecules (MW $<$ 500) following Lipinski's rules (*42*) was selected from the HitFinder Collection (Maybridge) (*43*). The library was purchased in 96-well plates, each containing one compound at a 4 mM concentration in DMSO, and it was stored frozen at -80 °C.

High-Throughput Screening. The thermal stability of Hp-Fld has been characterized in depth (*33, 39*). As the temperature is raised, the protein experiences three transitions, of which the lower temperature one is crucial because the FMN cofactor dissociates and the biological activity is lost. This transition can be conveniently monitored by following FMN emission fluorescence, which greatly increases upon dissociation (*33*). Screening for binders to Hp-Fld was performed in a FluoDia T70 spectrofluorimeter (Photal Otsuka electronics) following FMN fluorescence emission at 530 nm (excitation at 450 nm). The samples were located in 96-V-shape well plates (Thermo-Fast96 from ABgene), which were selected to ensure a homogeneous temperature distribution. The screening was performed in two steps. In the first one, five compounds were added, at a final 100 μM concentration each, to 5 μM Hp-Fld samples dissolved in 50 mM EPPS, pH 9.0. The final DMSO concentration in the assay solutions was 12.5% in a final assay volume of 200 μL. After mixing, each well was overlaid with 20 μL of mineral oil (Sigma-Aldrich) to prevent evaporation. Samples were incubated between 1 and 2 h at RT in the dark before fluorescence measurement. Reference control wells without compounds, and containing the same amount of DMSO and protein as the testing wells, were distributed on the plate, usually in rows 1 and 12. The unfolding curves corresponding to each well were analyzed using homemade software that estimates the midpoint temperature of unfolding (T_m) of each well, using two methods that we have termed "middle point" and "inflection point", designed to complement each other and to avoid false negatives. Details on these analyses will be reported elsewhere. The relevant compounds in the positive wells showing a clear increase in flavodoxin thermal stability ($\Delta T_m \geq 3$ °C) were identified in a second screening step by individual testing of compounds in final DMSO concentrations of 2.5%.

After HTS, confirmatory experiments were carried out by determining Hp-Fld thermal unfolding curves in the presence of ligand in 50 mM EPPS, pH 9.0, using an Aminco-Bowman Series 2 fluorimeter with excitation at 445 nm and emission at 525 nm. The curves were fit to a two-state model equation (*44*).

Affinities of Hp-Fld for Inhibitors and for FqrB. Ligand binding affinities can be estimated from the increases in protein stability induced by the ligands (*24, 27*). However, we determined more accurate affinity constants by isothermal titration calorimetry using a VP-ITC titration calorimeter (Microcal, Inc.). Flavodoxin solutions (20 μM) present in the calorimetric cell were titrated at 25.0 °C with inhibitor solutions (at initial concentrations of around 500 μM) dissolved in the same buffer (50 mM EPPS, pH 9.0 and 5% DMSO). Both solutions were previously degassed. The heat evolved after each injection was obtained from the integral of the calorimetric peak.

Flavodoxin binding to FqrB in 50 mM Tris, pH 8, was similarly followed by ITC. A 16 μM FqrB solution present in the calorimetric cell was titrated with 180 μM Hp-Fld. The influence of inhibitor III on the binding of Fld to FqrB was determined by including 300 μM inhibitor in both the syringe and the cell, which led to final DMSO concentrations of 1%. All samples were prepared and incubated for 30 min before the titration.

Electron Transfer Kinetics. The electron transfer activity of Hp-Fld was assayed in presence of its physiological redox partners PFOR and FqrB. Coupled enzyme reactions contained 0.15 mg mL^{-1} PFOR solution (around 0.4 μM PFOR), 3–5 μM Hp-Fld, and 0.15 μM FqrB in 100 mM potassium phosphate, pH 7.0, with 10 mM sodium pyruvate, 1 mM $MgCl_2$ and 300 μM $NADP^+$. Two conditions were used: pseudonanaerobic conditions, where a nitrogen flow was used to purge the oxygen excess in an ordinary absorbance cuvette; and strict anaerobic conditions, achieved using a specially designed anaerobic cuvette, coupled with an anaerobic train, where oxygen is removed by several cycles of vacuum and argon flow. Pseudoanaerobic kinetics were followed with a modified Cary-14 spectrophotometer equipped with an OLIS data as acquisition system (On Line Instrument Co., Bogart, GA) while anaerobic kinetics were followed by recording visible spectra in a diode array spectrophotometer (Agilent/HP 8453). All kinetics were performed at RT (25 $\pm$ 2 °C). The reactions were started by adding 0.18 mM of CoA, and NADPH formation was quantified using an extinction coefficient of 6.3 mM^{-1} cm^{-1} at 340 nm.

Minimal Inhibitory Concentration Determination and Bactericidal Assays. Hp-Fld strains 26695 and Hp1061 were grown in *Brucella*-based medium supplemented with 7.5% fetal bovine serum as previously described (*21*). *C. jejuni* strain H840 was also grown in *Brucella* medium without serum. All bacterial strains were grown in a humidified microaerobic incubator (85% N_2, 10% CO_2, 5% O_2) at 37 °C. For the microdilution MIC testing, 96 well round-bottom microtiter dishes were used. Bacteria were grown overnight in Brain Heart Infusion broth (BHI) supplemented with 2% serum. The bacteria were then diluted to an OD_{660} of 0.01 in BHI broth, and 200 μL of this inoculum and 2 μL of an appropriate concentration of test compound were dispensed into the first well of each row of 96-well plates, with 100 μL of inoculum added to the subsequent wells; then 2-fold serial dilutions were made along each row by mixing and sequentially transferring 100 μL from the first wells through the 11th. It was found that up to 3% (v/v) of the compound DMSO could be used in the assay without any deleterious effect, although concentrations $>$3% were inhibitory to growth. Plates were incubated under microaerobic conditions with shaking at 100 rpm and examined visually after 28 h. The lowest compound concentration to cause complete inhibition of growth was recorded as the MIC.

For bactericidal determination, bacteria were diluted in BHI broth supplemented with 2% newborn calf serum to an OD_{660} of 0.1. A volume of 7.5 μL of appropriate test compound was dispensed in 3 mL of BHI to give a final test concentration of 2$\times$ MIC in 0.25% DMSO. Plates were incubated under microaerobic conditions with shaking. At each time point, a 0.3 mL aliquot was removed, centrifuged to remove residual test compound, and suspended in BHI broth, and decimal dilutions were plated on *Brucella* agar supplemented with 7.5% serum for determination of viable counts. Bactericidal activity was calculated following comparison with the DMSO control.

Conflict of Interest: N.C., A.V.-C., and J.S. have a patent pending on the use of Inhibitors I–IV in the treatment of HP infection.

Acknowledgment: We acknowledge financial support from grants BFU2007-61476/BMC, CTQ2005-00360, SAF2008-05742-C02-01 (to J.L.N.) and CSD-2008-00005 (to J.L.N.) from Spanish Ministerio de Educación y Ciencia (MEC), grant PI078/08 from Gobierno de Aragón (Spain), grant 2008/0670 from Genoma España, grant FIPSE (Exp 36557/06) to J.L.N., and NIH grants R01DK073823 and U01AI075520 to P.S.H. N.C. and I.P.-D. were supported by FPU and I3P-CSIC fellowships (Spain), respectively. We acknowledge help from F.J. Castillo and R. Benito in early stages of the work.

Supporting Information Available: This material is free of charge *via* the Internet at http://pubs.acs.org.

REFERENCES

1. Marshall, B. J., and Warren, J. R. (1984) Unidentified curved bacilli in the stomach of patients with gastritis and peptic ulceration, *Lancet 1*, 1311–1315.
2. Wotherspoon, A. C., Doglioni, C., Diss, T. C., Pan, L., Moschini, A., de Boni, M., and Isaacson, P. G. (1993) Regression of primary low-grade B-cell gastric lymphoma of mucosa-associated lymphoid tissue type after eradication of *Helicobacter pylori*, *Lancet 342*, 575–577.
3. Parsonnet, J., Hansen, S., Rodriguez, L., Gelb, A. B., Warnke, R. A., Jellum, E., Orentreich, N., Vogelman, J. H., and Friedman, G. D. (1994) Helicobacter pylori infection and gastric lymphoma, *N. Engl. J. Med. 330*, 1267–1271.
4. Parsonnet, J., Friedman, G. D., Vandersteen, D. P., Chang, Y., Vogelman, J. H., Orentreich, N., and Sibley, R. K. (1991) *Helicobacter pylori* infection and the risk of gastric carcinoma, *N. Engl. J. Med. 325*, 1127–1131.
5. Bruce, M. G., and Maaroos, H. I. (2008) Epidemiology of *Helicobacter pylori* infection, *Helicobacter 13*, 1–6.
6. Wilson, K. T., and Crabtree, J. E. (2007) Immunology of *Helicobacter pylori*: insights into the failure of the immune response and perspectives on vaccine studies, *Gastroenterology 133*, 288–308.
7. Agarwal, K., and Agarwal, S. (2008) Helicobacter pylori vaccine: from past to future, *Mayo Clin. Proc. 83*, 169–175.
8. Seppala, K., and Nuutinen, H. (1995) New options in eradication of *Helicobacter pylori*, *Ann. Med. 27*, 601–604.
9. Adamek, R. J., Suerbaum, S., Pfaffenbach, B., and Opferkuch, W. (1998) Primary and acquired *Helicobacter pylori* resistance to clarithromycin, metronidazole, and amoxicillin—influence on treatment outcome, *Am. J. Gastroenterol. 93*, 386–389.
10. Glupczynski, Y. (1998) Antimicrobial resistance in *Helicobacter pylori*: a global overview, *Acta Gastroenterol. Belg. 61*, 357–366.
11. Ferrero, M., Ducons, J. A., Sicilia, B., Santolaria, S., Sierra, E., and Gomollon, F. (2000) Factors affecting the variation in antibiotic resistance of *Helicobacter pylori* over a 3-year period, *Int. J. Antimicrob. Agents 16*, 245–248.
12. Wu, J. Y., Kim, J. J., Reddy, R., Wang, W. M., Graham, D. Y., and Kwon, D. H. (2005) Tetracycline-resistant clinical *Helicobacter pylori* isolates with and without mutations in 16S rRNA-encoding genes, *Antimicrob. Agents Chemother. 49*, 578–583.
13. Carothers, J. J., Bruce, M. G., Hennessy, T. W., Bensler, M., Morris, J. M., Reasonover, A. L., Hurlburt, D. A., Parkinson, A. J., Coleman, J. M., and McMahon, B. J. (2007) The relationship between previous fluoroquinolone use and levofloxacin resistance in *Helicobacter pylori* infection, *Clin. Infect. Dis. 44*, e5–8.
14. Graham, D. Y., and Shiotani, A. (2008) New concepts of resistance in the treatment of *Helicobacter pylori* infections, *Nat. Clin. Pract. Gastroenterol. Hepatol. 5*, 321–331.
15. Mégraud, F. (2004) Basis for the management of drug-resistant *Helicobacter pylori* infection, *Drugs 64*, 1893–1904.
16. Chalker, A. F., Minehart, H. W., Hughes, N. J., Koretke, K. K., Lonetto, M. A., Brinkman, K. K., Warren, P. V., Lupas, A., Stanhope, M. J., Brown, J. R., and Hoffman, P. S. (2001) Systematic identification of selective essential genes in *Helicobacter pylori* by genome prioritization and allelic replacement mutagenesis, *J. Bacteriol. 183*, 1259–1268.
17. Freigang, J., Diederichs, K., Schafer, K. P., Welte, W., and Paul, R. (2002) Crystal structure of oxidized flavodoxin, an essential protein in *Helicobacter pylori*, *Protein Sci. 11*, 253–261.
18. Cremades, N., Bueno, M., Toja, M., and Sancho, J. (2005) Towards a new therapeutic target: *Helicobacter pylori* flavodoxin, *Biophys. Chem. 115*, 267–276.
19. Sancho, J. (2006) Flavodoxins: sequence, folding, binding, function and beyond, *Cell. Mol. Life Sci. 63*, 855–864.
20. Hughes, N. J., Chalk, P. A., Clayton, C. L., and Kelly, D. J. (1995) Identification of carboxylation enzymes and characterization of a novel four-subunit pyruvate:flavodoxin oxidoreductase from *Helicobacter pylori*, *J. Bacteriol. 177*, 3953–3959.
21. St Maurice, M., Cremades, N., Croxen, M. A., Sisson, G., Sancho, J., and Hoffman, P. S. (2007) Flavodoxin:Quinone Reductase (FqrB): a redox partner of pyruvate:ferredoxin oxidoreductase that reversibly couples pyruvate oxidation to NADPH production in *Helicobacter pylori* and *Campylobacter jejuni*, *J. Bacteriol. 189*, 4764–4773.
22. Baker, L. M., Raudonikiene, A., Hoffman, P. S., and Poole, L. B. (2001) Essential thioredoxin-dependent peroxiredoxin system from *Helicobacter pylori*: genetic and kinetic characterization, *J. Bacteriol. 183*, 1961–1973.
23. Pace, C. N., and McGrath, T. (1980) Substrate stabilization of lysozyme to thermal and guanidine hydrochloride denaturation, *J. Biol. Chem. 255*, 3862–3865.
24. Brandts, J. F., and Lin, L. N. (1990) Study of strong to ultratight protein interactions using differential scanning calorimetry, *Biochemistry 29*, 6927–6940.
25. Straume, M., and Freire, E. (1992) Two-dimensional differential scanning calorimetry: simultaneous resolution of intrinsic protein structural energetics and ligand binding interactions by global linkage analysis, *Anal. Biochem. 203*, 259–268.
26. Pantoliano, M. W., Petrella, E. C., Kwasnoski, J. D., Lobanov, V. S., Myslik, J., Graf, E., Carver, T., Asel, E., Springer, B. A., Lane, P., and Salemme, F. R. (2001) High-density miniaturized thermal shift assays as a general strategy for drug discovery, *J. Biomol. Screening 6*, 429–440.
27. Lo, M. C., Aulabaugh, A., Jin, G., Cowling, R., Bard, J., Malamas, M., and Ellestad, G. (2004) Evaluation of fluorescence-based thermal shift assays for hit identification in drug discovery, *Anal. Biochem. 332*, 153–159.
28. Senisterra, G. A., Markin, E., Yamazaki, K., Hui, R., Vedadi, M., and Awrey, D. E. (2006) Screening for ligands using a generic and high-throughput light-scattering-based assay, *J. Biomol. Screening 11*, 940–948.
29. Grasberger, B. L., Lu, T., Schubert, C., Parks, D. J., Carver, T. E., Koblish, H. K., Cummings, M. D., LaFrance, L. V., Milkiewicz, K. L., Calvo, R. R., Maguire, D., Lattanze, J., Franks, C. F., Zhao, S., Ramachandren, K., Bylebyl, G. R., Zhang, M., Manthey, C. L., Petrella, E. C., Pantoliano, M. W., Deckman, I. C., Spurlino, J. C., Maroney, A. C., Tomczuk, B. E., Molloy, C. J., and Bone, R. F. (2005) Discovery and cocrystal structure of benzodiazepinedione HDM2 antagonists that activate p53 in cells, *J. Med. Chem. 48*, 909–912.
30. Matulis, D., Kranz, J. K., Salemme, F. R., and Todd, M. J. (2005) Thermodynamic stability of carbonic anhydrase: measurements of binding affinity and stoichiometry using ThermoFluor, *Biochemistry. 44*, 5258–5266.
31. Pey, A. L., Ying, M., Cremades, N., Velazquez-Campoy, A., Scherer, T., Thony, B., Sancho, J., and Martinez, A. (2008) Identification of pharmacological chaperones as potential therapeutic agents to treat phenylketonuria, *J. Clin. Invest. 118*, 2858–2867.

32. Tucker, C. L. (2002) High-throughput cell-based assays in yeast, *Drug Discovery Today 7*, S125–130.
33. Cremades, N., Velazquez-Campoy, A., Freire, E., and Sancho, J. (2008) The flavodoxin from *Helicobacter pylori*: structural determinants of thermostability and FMN cofactor binding, *Biochemistry 47*, 627–639.
34. Hoffman, P. S., Sisson, G., Croxen, M. A., Welch, K., Harman, W. D., Cremades, N., and Morash, M. G. (2007) Antiparasitic drug nitazoxanide inhibits the pyruvate oxidoreductases of *Helicobacter pylori* and selected anaerobic bacteria and parasites, and *Campylobacter jejuni*, *Antimicrob. Agents Chemother. 51*, 868–876.
35. Piccolomini, R., Di Bonaventura, G., Picciani, C., Laterza, F., Vecchiet, J., and Neri, M. (2001) In vitro activity of clarithromycin against intracellular *Helicobacter pylori*, *Antimicrob. Agents Chemother. 45*, 1568–1571.
36. Fotakis, G., and Timbrell, J. A. (2006) In vitro cytotoxicity assays: comparison of LDH, neutral red, MTT and protein assay in hepatoma cell lines following exposure to cadmium chloride, *Toxicol. Lett. 160*, 171–177.
37. Abraham, V. C., Towne, D. L., Waring, J. F., Warrior, U., and Burns, D. J. (2008) Application of a high-content multiparameter cytotoxicity assay to prioritize compounds based on toxicity potential in humans, *J. Biomol. Screening 13*, 527–537.
38. Kover, K. E., Groves, P., Jimenez-Barbero, J., and Batta, G. (2007) Molecular recognition and screening using a 15N group selective STD NMR method, *J. Am. Chem. Soc. 129*, 11579–11582.
39. Cremades, N., Bueno, M., Neira, J. L., Velazquez-Campoy, A., and Sancho, J. (2008) Conformational stability of *Helicobacter pylori*flavodoxin: fit to function at pH 5, *J. Biol. Chem. 283*, 2883–2895.
40. Sisson, G., Goodwin, A., Raudonikiene, A., Hughes, N. J., Mukhopadhyay, A. K., Berg, D. E., and Hoffman, P. S. (2002) Enzymes associated with reductive activation and action of nitazoxanide, nitrofurans, and metronidazole in H*elicobacter pylori*, *Antimicrob. Agents Chemother. 46*, 2116–2123.
41. Mayhew, S. G., and Massey, V. (1969) Purification and characterization of flavodoxin from *Peptostreptococcus elsdenii*, *J. Biol. Chem. 244*, 794–802.
42. Lipinski, C. A., Lombardo, F., Dominy, B. W., and Feeney, P. J. (2001) Experimental and computational approaches to estimate solubility and permeability in drug discovery and development settings, *Adv. Drug Delivery Rev. 46*, 3–26.
43. McGregor, M. J., and Pallai, P. V. (1997) Clustering of large databases of compounds: using the MDL "keys" as structural descriptors, *J. Chem. Inf. Comput. Sci. 37*, 443–448.
44. Privalov, P. L. (1979) Stability of proteins: small globular proteins, *Adv. Protein Chem. 33*, 167–241.